Inorg. Chem. **2009**, *48*, 2443−2448

Inorganic Chemistry
Article

Spin-State Crossover with Structural Changes in a Cobalt(II) Organometallic Species: Low-Coordinate, First Row, Heteroleptic Amido Transition Metal Aryls. Synthesis and Characterization of Ar′MN(H)Ar# (M = Mn, Fe, Co) (Ar′ = C_6H_3-2,6-(C_6H_3-2,6-$^iPr_2$)$_2$, Ar# = C_6H_3-2,6-(C_6H_2-2,4,6-Me_3)$_2$)

Chengbao Ni,[†] James C. Fettinger,[†] Gary J. Long,[‡] and Philip P. Power*,[†]

Department of Chemistry, University of California, Davis, One Shields Avenue, California 95616, and Department of Chemistry, Missouri University of Science and Technology, Rolla, Missouri 65409

Received September 3, 2008

The synthesis and characterization of the monomeric aryl transition metal amido complexes Ar′MN(H)Ar# (Ar′ = C_6H_3-2,6-(C_6H_3-2,6-$^iPr_2$)$_2$, Ar# = C_6H_3-2,6-(C_6H_2-2,4,6-Me_3)$_2$, M = Mn (**1**), Fe (**2**), Co(**3a, b**)) are reported. The compounds were characterized by X-ray crystallography, electronic and infrared spectroscopy, and magnetic measurements. At about 90 K the complexes **1** and **2** possess quasi-two coordinate geometry with a weak, secondary, M---C interaction involving a flanking aryl ring from an amido group. In contrast, at the same temperature, their cobalt analogue **3a** features a strong Co-η^6-flanking ring interaction to give an effectively higher coordination geometry. Magnetic studies of **1**−**3a** showed that **1** and **2** have high spin configurations, whereas the cobalt species **3a** has a low-spin configuration ($S = 1/2$). However, **3a** undergoes a spin crossover to a high spin ($S = 3/2$) state **3b** near 229 K. An X-ray structural determination above the crossover temperature at 240 K showed that the low temperature structure of **3a** had changed to **3b** which involves a weak secondary M---C interaction analogous to those in **1** and **2**. The complexes **1**−**3** are very rare examples of heteroleptic quasi-two coordinate open shell transition metal complexes.

Introduction

Amido complexes of transition metals[1] are attracting increased attention as supporting ligands for molecular catalysts[2−14] and for their involvement as important intermediates in many catalytic processes.[8,15−22] They are also of inherent interest because of the ability of the amido ligand (-NR_2) to combine steric flexibility, good metal−ligand bond strength, and relatively straightforward synthetic accessibility. This enables a wide variety of complexes with unusual bonding modes and coordination numbers to be isolated.[1] These attributes led to their pioneering use in the synthesis of low (2 or 3) coordinate open shell (d^1-d^9) complexes.[23−27]

* To whom correspondence should be addressed. E-mail: pppower@ucdavis.edu. Fax: (+01) 530-752-8995.
† University of California, Davis.
‡ Missouri University of Science and Technology.

(1) Lappert, M. F.; Power, P. P.; Sanger, A. R.; Srivastava, R. C. *Metal and Metalloid Amides*: Ellis Horwood, Chichester, U.K., 1980.
(2) (a) Fryzuk, M. D.; Montgomery, C. D. *Coord. Chem. Rev.* **1989**, *95*, 1. (b) MacLachlan, E. A.; Fryzuk, M. D. *Organometallics* **2006**, *25*, 1530.
(3) Roundhill, D. M. *Chem. Rev.* **1992**, *92*, 1.
(4) Schrock, R. R. *Acc. Chem. Res.* **1997**, *30*, 9.
(5) Cummins, C. C. *Chem. Commun.* **1998**, 1777.
(6) Gade, L. H.; Mountford, P. *Coord. Chem. Rev.* **2001**, *65*, 216.
(7) McKnight, A. L.; Waymouth, R. M. *Chem. Rev.* **1998**, *98*, 2587.
(8) Britovsek, G. J.; Gibson, P. V. C.; Wass, D. F. *Angew. Chem., Int. Ed.* **1999**, *38*, 428.
(9) Gade, L. H. *Chem. Commun.* **2000**, 173.
(10) Kempe, R. *Angew. Chem., Int. Ed.* **2000**, *39*, 468.
(11) Caro, C. F.; Lappert, M. F.; Merle, P. G. *Coord. Chem. Rev.* **2001**, *219*−*221*, 605.
(12) Gibson, V. C.; Spitzmesser, S. K. *Chem. Rev.* **2003**, *103*, 283.
(13) Gambarotta, S.; Scott, J. *Angew. Chem., Int. Ed.* **2004**, *43*, 5298.
(14) Liang, L.-C. *Coord. Chem. Rev.* **2006**, *250*, 1152.
(15) Bryndza, H. E.; Tam, W. *Chem. Rev.* **1988**, *88*, 1163.
(16) Hartwig, J. F. *Angew. Chem., Int. Ed.* **1998**, *37*, 2046.
(17) McKnight, A. L.; Waymouth, R. M. *Chem. Rev.* **1998**, *98*, 2587.
(18) Holland, P. L.; Andersen, R. A.; Bergman, R. G. *Comments Inorg. Chem.* **1999**, *21*, 115.
(19) Fulton, J. R.; Holland, A. W.; Fox, D. J.; Bergman, R. G. *Acc. Chem. Res.* **2002**, *35*, 44.
(20) Schrock, R. R. *Acc. Chem. Res.* **2005**, *38*, 955.
(21) Mindiola, D. J. *Acc. Chem. Res.* **2006**, *39*, 813.
(22) Gunnoe, T. B. *Eur. J. Inorg. Chem.* **2007**, 1185.

10.1021/ic801660a CCC: $40.75
Published on Web 02/12/2009

For example, the use of sterically encumbering amido ligands has permitted the synthesis of several stable two-coordinate derivatives of Cr, Mn, Fe, Co, and Ni.[28,29] Analogous complexes involving other bulky ligands such as alkyls or aryls are rare. The first stable, open-shell, two coordinate organometallic species in the solid state was the dialkyl $Mn(C(SiMe_3)_3)_2$.[30] The corresponding iron compound $Fe(C(SiMe_3)_3)_2$[31] has also been reported. The use of the bulky aryl ligand Mes* (Mes* = C_6H_2-2,4,6-$^tBu_3$) permitted this class of compounds to be extended to include $MMes^*_2$ (M = Mn,[32] or Fe[32,33]) and more recently the terphenyl ligand $Ar^{\#}(C_6H_3$-2,6-$Mes_2)$ has been used to stabilize the complexes $MAr^{\#}_2$ (M = Mn - Co).[34] A feature of these amido, alkyl or aryl derivatives is that they are homoleptic. Currently there are very few examples of heteroleptic two coordinate complexes and they are limited to $((Me_3Si)_2N)Fe(SAr^{\#})$[35] and the recently reported $Fe(SAr^{\#})\{SC_6H_3$-2,6-$(SiMe_3)_2\}$[36] and Cr(1) complex $(L)Cr(C_6H$-2,6-$(C_6H_2$-2,4,6-$^iPr_3)_2$-3,5-$^iPr_2)$ (L = THF or PMe_3).[37] A major obstacle to the synthesis of the heteroleptic complexes is the scarcity of suitable starting materials that would afford two-coordinate complexes upon derivatization with amido or organo groups. However, the recent isolation of well characterized monoaryl transition metal halides of the formula $(Ar'MX)_2$ (M = Cr, X = Cl, $Ar' = C_6H_3$-2,6-$(C_6H_3$-2,6-$^iPr_2)_2)$ or $((Et_2O)Li)_2Mn_2Ar'_2I_4$ (M = Mn, Fe, Co)[38] has provided suitable building blocks for low-coordinate heteroleptic species. Here we report the synthesis and characterization of a series of heteroleptic complexes Ar′MN(H)Ar# (M = Mn (**1**), Fe(**2**), Co(**3**)) stabilized by bulky terphenyl and primary arylamido ligands.

Experimental Section

General Procedures. All manipulations were carried out using modified Schlenk techniques under an argon atmosphere or in a Vacuum Atmospheres HE-43 drybox. All of the solvents were dried over an aluminum column, stored over 3 Å molecular sieves overnight, and degassed three times (freeze−thaw) prior to use. The metal halide precursors[38] and $Ar^{\#}N(H)Li$[39] were prepared according to literature procedures. Melting points were recorded in glass capillaries sealed under N_2 and are uncorrected. UV−vis data were recorded on a Hitachi-1200 spectrometer.

Ar′MnN(H)Ar#·0.5 *n*-hexane (1·0.5 *n*-hexane). About 30 mL of hexanes was added to a mixture of $[Li(THF)Ar'MnI_2]_2$ (0.393 g, 0.25 mmol) and $LiN(H)Ar^{\#}$ (0.171 g, 0.51 mmol) at room temperature. The mixture was stirred for 1 day by which time the solution had become light yellow and some white precipitate had formed. The solution was filtered, and the light yellow filtrate was concentrated to about 5 mL, which afforded X-ray quality pale yellow crystals of **1** after storage for 4 days at −18 °C. Yield 0.248 g (63.4%). mp 163−165 °C. UV−vis (hexane, nm [ε, $cm^{-1}\,M^{-1}$]): 382(700).

Ar′FeN(H)Ar# (2). About 30 mL of hexanes was added to a mixture of $[Ar'Fe(\mu\text{-Br})]_2$ (0.267 g, 0.25mmol) and $LiN(H)Ar^{\#}$ (0.171 g, 0.51mmol) at room temperature. The amber solution had become red in 2 h. The mixture was stirred for 1 day by which time the solution had become bright red and some white precipitate had formed. The solution was filtered and the bright red filtrate was concentrated to about 5 mL, which afforded X-ray quality bright red crystals of **2** after storage for overnight at −18 °C. Yield 0.285 g (73.0%). mp 110 °C(dec). Anal. Calcd. For $C_{54}H_{63}FeN$: C, 82.94; H, 8.12; N, 1.79; Found: C, 81.8, H, 7.89; N, 1.754.UV−vis (hexane, nm [ε, $cm^{-1}\,M^{-1}$]): 450(2500).

Ar′CoN(H)Ar# (3a and 3b). About 30 mL of hexanes was added to a mixture of $[Ar'Co(\mu\text{-Cl})]_2$ (0.246 g, 0.25mmol) and $LiN(H)Ar^{\#}$ (0.171 g, 0.51mmol) at room temperature. The orange brown solution became deep purple after about 30 min. The mixture was stirred for 1 day by which time the solution had become deep purple and a white precipitate had formed. The solution was filtered and the deep purple filtrate was concentrated to ca. 15 mL, which afforded X-ray quality dark purple crystals of **3** after storage for overnight at 7 °C. Yield 0.289 g (68.5%). mp 174−177 °C. Anal. Calcd. for $C_{54}H_{63}CoN$: C, 82.62; H, 8.09; N, 1.78. Found: C, 81.91; H, 8.0; N, 1.76. UV−vis (hexane, nm [ε, $cm^{-1}\,M^{-1}$]): 548(3400) and 696(1400).

X-ray Crystallographic Studies. Suitable crystals of **1**−**3a** and **3b** were selected and covered with a layer of hydrocarbon oil under a rapid flow of argon. They were mounted on a glass fiber attached to a copper pin and placed in the cold N_2 stream on the diffractometer. For **1** and **2**, X-ray data were collected on a Bruker SMART 1000 diffractometer at 90(2) K using Mo Kα radiation (λ = 0.71073 Å), while for **3**, X-ray data were collected on a Bruker SMART Apex II diffractometer at both 90(2) and 240(2) K using Mo K radiation (λ = 0.71073 Å). Absorption corrections were applied using SADABS.[40] The structures were solved using direct methods and refined by the full-matrix least-squares procedure in SHELX.[41] All of the non-hydrogen atoms were refined anisotropically. The hydrogen atom on the nitrogen in all three compounds was located by use of a Fourier difference map, and the other hydrogens in each structure were placed at calculated positions and included in the refinement using a riding model.

Magnetic Studies. The samples for magnetization measurements were sealed under vacuum in 3 mm quartz tubing. The sample magnetization was measured using a Quantum Designs MPMSXL7 superconducting quantum interference device (SQUID) magnetometer. For each measurement, the sample was zero-field cooled to 2 K, and the magnetization was measured in 0.5 K increments to 4 K, 1 K increments to 10 K, 1.5 K increments to 24 K, 5 K increments to 70 K, and 10 K increments to 320 K under constant field of either 0.001 T or 0.01 T and with a long delay time.

(23) Bradley, D. C. *Chem. Br.* **1975**, *11*, 393.
(24) Bradley, D. C.; Chisholm, M. H. *Acc. Chem. Res.* **1976**, *9*, 273.
(25) Eller, P. G.; Bradley, D. C.; Hursthouse, M. B.; Meek, D. W. *Coord. Chem. Rev.* **1977**, *24*, 1.
(26) Cummins, C. C. *Prog. Inorg. Chem.* **1998**, *47*, 685.
(27) Alvarez, S. *Coord. Chem. Rev.* **1999**, *13*, 193.
(28) Power, P. P. *Comments Inorg. Chem.* **1989**, *8*, 177.
(29) Power, P. P. *Chemtracts: Inorg. Chem.* **1994**, *6*, 181.
(30) (a) Buttrus, N. H.; Eaborn, C.; Hitchcock, P. B.; Smith, J. D.; Sullivan, A. C. *Chem. Commun.* **1985**, 1380. (b) Viefhaus, T.; Schwarz, W.; Hubler, K.; Locke, K.; Weidlein, J. *Z. Anorg. Allg. Chem.* **2001**, *627*, 715.
(31) LaPointe, A. M. *Inorg. Chim. Acta* **2003**, *345*, 359.
(32) Wehmschulte, R. J.; Power, P. P. *Organometallics* **1995**, *14*, 3264.
(33) Muller, H.; Seidel, W.; Gorls, H. *Angew. Chem., Int. Ed. Engl.* **1995**, *34*, 325.
(34) Kays, D. L.; Cowley, A. R. *Chem. Commun.* **2007**, 1053.
(35) Ellison, D. J.; Ruhlandt-Senge, K.; Power, P. P. *Angew. Chem., Int. Ed. Engl.* **1994**, *33*, 1178.
(36) Ohta, S.; Ohki, Y.; Ikagawa, Y.; Suizu, R.; Tatsumi, K. *J. Organomet. Chem.* **2007**, *692*, 4792.
(37) Wolf, R.; Brynda, M.; Ni, C.; Long, G. J.; Power, P. P. *J. Am. Chem. Soc.* **2007**, *129*, 6076.
(38) Sutton, A. D.; Nguyen, T.; Fettinger, J. C.; Olmstead, M. M.; Long, G. J.; Power, P. P. *Inorg. Chem.* **2007**, *46*, 4809.
(39) Gavenonis, J.; Tilley, T. D. *Organometallics* **2002**, *21*, 5549.
(40) *SADABS, version 5.0 package; an empirical absorption correction program from the SAINTPlus NT*; Bruker AXS: Madison, WI, 1998.
(41) *SHELXL, version 5.1*; Bruker AXS: Madison, WI, 1998.

Scheme 1. Synthesis of Aryl Metal Amido Complexes **1**−**3**

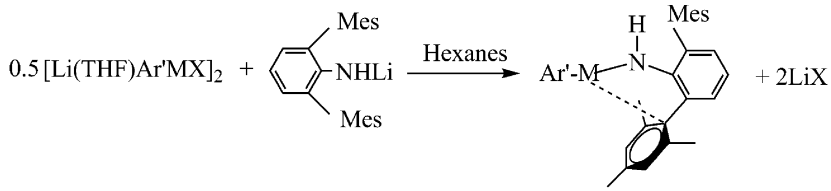

1, M = Mn, X = I; **2,** M = Fe, X = Br

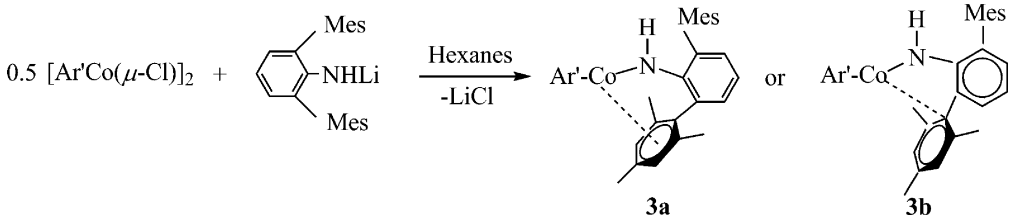

Table 1. Selected Crystallographic Data and Collection Parameters for **1**−**3**[a]

	1·0.5 *n*-hexane	**2**	**3a**	**3b**
formula	$C_{57}H_{70}MnN$	$C_{54}H_{63}FeN$	$C_{64}H_{63}CoN$	$C_{64}H_{63}CoN$
fw	824.08	781.90	784.98	784.98
color, habit	pale yellow, plate	red, block	deep purple, block	deep purple, block
cryst syst	triclinic	monoclinic	monoclinic	monoclinic
space group	$P\bar{1}$	$P2_1/c$	$P2_1/c$	$P2_1/c$
a, Å	10.6554(7)	19.6531(13)	19.962(5)	19.9318(9)
b, Å	12.5210(8)	11.4831(7)	11.288(3)	11.5995(5)
c, Å	20.2032(13)	19.8523(13)	19.485(5)	19.6369(9)
α, deg	75.825(1)	90	90	90
β, deg	82.460(1)	99.605(1)	103.042(4)	99.932(1)
γ, deg	68.015(1)	90	90	90
V, Å^3	2421.0(3)	4417.4(5)	4277.5(18)	4472.0(3)
Z	2	4	4	4
d_{calcd}, Mg/m^3	1.13	1.176	1.219	1.166
θ range, deg	1.04−27.5	1.05−27.55	2.76−25.25	2.72−27.18
μ, mm^{-1}	0.309	0.378	0.439	0.419
obs data, $I > 2\sigma(I)$	9745	8870	6657	7689
R1(obs data)	0.0405	0.0338	0.0576	0.0382
*w*R2(all data)	0.1218	0.0988	0.1479	0.1108

[a] **3a** was collected at 90 K, **3b** was collected at 240 K.

Results and Discussion

Synthesis and Spectroscopy. Reaction of Ar$^{\#}$N(H)Li with half an equivalent of the terphenyl metal halides [Li(THF)Ar′MnI$_2$]$_2$, [Ar′Fe(*μ*-Br)]$_2$, or [Ar′Co(*μ*-Cl)]$_2$ in hexanes at room temperature yielded the aryl metal amido complexes **1**−**3** according to Scheme 1. The complexes **1**−**3** could be isolated from hexanes as very air and moisture sensitive pale yellow, bright red, or deep purple crystals, respectively. They can be stored at room temperature under an inert atmosphere for several months.

The UV−visible spectra of **1**−**3** are characterized by intense absorptions below 250 nm corresponding to *π*-*π** transitions within the terphenyl ligand. In addition, **1** features a low-intensity absorption centered at 382 nm ($\varepsilon = 700$ cm^{-1} M^{-1}), and has a featureless spectrum in the visible region, which is as expected for a high-spin d^5 system. Compound **2** displays a relatively intense absorption centered at 450 nm ($\varepsilon = 2500$ cm^{-1} M^{-1}) and **3** shows very broad absorptions at 548 nm ($\varepsilon = 3400$ cm^{-1} M^{-1}) and 696 nm ($\varepsilon = 1400$ cm^{-1} M^{-1}). In their infrared spectra, the N−H stretching absorptions are very similar for all 3 compounds and are observed near 3390 cm^{-1}.

Table 2. Selected Bond Lengths (Å) and Angles (deg)

	1·0.5*n*-hexane	**2**	**3a**	**3b**
M−C(*ipso*)	2.0953(13)	2.0455(13)	1.977(1)	1.992(2)
M−N	1.9807(12)	1.9324(12)	1.875(3)	1.880(2)
M−C(37)	2.5945(13)	2.4567(12)	2.077(3)	2.393(2)
Co−arene			2.150(3), 2.157(3)	2.519(2), 2.692(2)
			2.211(3), 2.220(3)	2.920(2), 3.049(2)
			2.143(3)	3.190(2)
N−C31	1.3733(17)	1.3768(16)	1.385(4)	1.374(2)
C32−C37	1.5009(18)	1.4889(18)	1.490(4)	1.488(2)
C36−C46	1.4964(19)	1.4966(17)	1.493(4)	1.493(2)
C1−M−N1	132.58(5)	134.97(5)	101.75(11)	133.90(6)
C1−M−C37	152.62(5)	149.25(4)		142.22(6)
M−N1−C31	126.35(9)	125.82(9)	118.0(2)	124.57(11)
C31−C32−C37	119.75(12)	115.24(11)	112.2(3)	116.24(13)

Structures. The structures of compounds **1**−**3** were determined by X-ray crystallography. Important data collection and refinement parameters for **1**−**3** are provided in Table 1, and selected structural data are given in Table 2. The crystals of **1**, **2**, and **3a** (at 240(2) K) are isomorphous, and their structures are very similar as illustrated in Figures 1, 2, and 3b. They feature quasi two-coordinate metal centers bonded to the *ipso*-carbon of the aryl and the nitrogen of the primary arylamido ligand, respectively. In addition, the

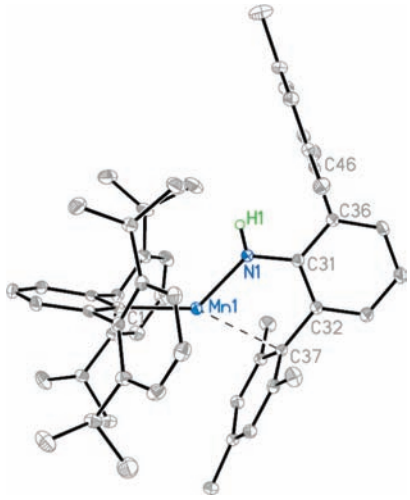

Figure 1. Molecular structure of **1** at 90 Kwith thermal ellipsoids presented at a 30% probability level. Hydrogen (except N−H) atoms are not shown for clarity.

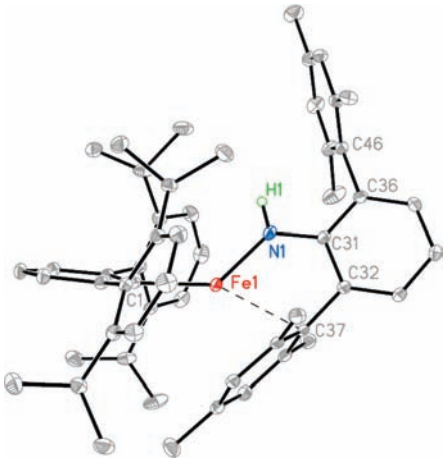

Figure 2. Molecular structure of **2** at 90 K with thermal ellipsoids presented at a 30% probability level. Hydrogen (except N−H) atoms are not shown for clarity.

metal centers interact with the *ipso* carbon (C(37)) of a flanking -C_6H_2-2,4,6-Me_3 ring from the arylamido ligand.

In **1,** the Mn−C(1) σ-bonded distance (2.0953(13) Å) is essentially the same as those in the aryl Mn(II) complexes $MnAr^{\#}_2$ (2.095(3) Å)[34] and $MnMes^*_2$ (2.108(2) Å).[32] The Mn−N distance (1.9807(12) Å) is similar to those in the amido complex $Mn(N(SiMePh_2)_2)_2$ (1.989(3) Å),[42] but somewhat shorter than those in $Mn(N(Mes)B(Mes)_2)_2$ (2.046(4) Å),[43] possibly as a result a weakened Mn−N bond because of multiple bonding between the boron and nitrogen atoms. The C(1)−Mn−N angle of 132.58(5)° deviates from linearity because of the interaction between Mn(II) and the *ipso* carbon(C(37)) of the flanking -C_6H_2-2,4,6-Me_3 ring. The Mn---C(37) distance is 2.5945(13) Å, is about 0.5 Å longer than the Mn−C(1) bond length, and is similar to the 2.536(5) Å observed in $Mn(N(Mes)B(Mes)_2)_2$.[43] Both of the Mn−C interactions in **1** may be compared to 2.37 Å predicted from the sum of their covalent radii.[44]

The structure of **2** is similar to that of **1**. The iron is similarly coordinated to the terphenyl ligand, the arylamido ligand, and also interacts with the *ipso* carbon(C(37)) of the flanking -C_6H_2-2,4,6-Me_3 ring. The Fe−C(1) distance of

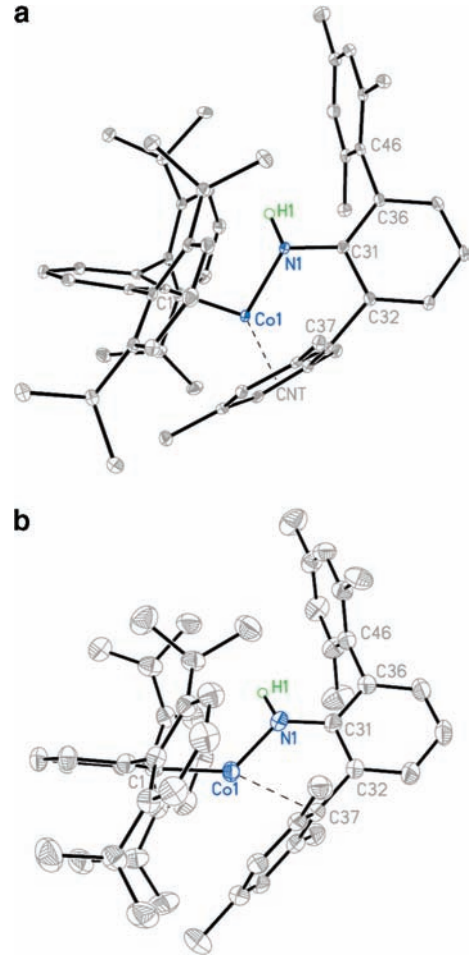

Figure 3. (a) Molecular structure of **3a** at 90 K with thermal ellipsoids presented at a 30% probability level. Hydrogen (except N−H) atoms are not shown for clarity. (b) Molecular structure of **3b** at 240 K with thermal ellipsoids presented at a 30% probability level. Hydrogen (except N−H) atoms are not shown for clarity.

2.0455(13) Å is comparable to those in $FeAr^{\#}_2$ (2.040(3) Å)[34] and $FeMes^*_2$ (2.058(6)Å).[32,33] The Fe−N distance (1.9324(12) Å) is similar to those amido complexes, such as Fe(N-(Mes)B$(Mes)_2)_2$ (1.938(2) Å)[45] and $Fe(N(SiMePh_2)_2)_2$ (1.917(2) Å).[46] The C(1)−Fe−N angle is 134.97(5)°, which is more than 30° narrower than those of 166.1(1) and 169.0(1)° in $Fe(N(Mes)B(Mes)_2)_2$[45] and $Fe[N(SiMePh_2)_2]_2$.[45] The Fe---C(37) distance (2.4567(12) Å) is about 0.5 Å longer than the Fe−C(1) bond length and is similar to that in $(Me_3Si)_2NFeSAr^{\#}$ (2.457 Å),[35] but is somewhat shorter than the interactions observed in $Fe(N(Mes)B(Mes)_2)_2$ (2.521 Å)[45] and $Fe(N(SiMePh_2)_2)_2$ (2.695(4) Å).[46] This might be due to the fact that in these examples, each Fe(II) center interacts with two aromatic rings, while in **2**, the Fe(II) center only interacts with one ring.

(42) Chen, H.; Bartlett, R. A.; Dias, H. V. R.; Olmstead, M. M.; Power, P. P. *J. Am. Chem. Soc.* **1989**, *111*, 4338.
(43) Bartlett, R. A.; Feng, X.; Olmstead, M. M.; Power, P. P.; Weese, K. J. *J. Am. Chem. Soc.* **1987**, *109*, 4851.
(44) Cardeno, B.; Gómez, V.; Platero-Prats, A. E.; Rves, M.; Echeveria, J.; Cremades, E.; Barragán, F.; Alvarez, S. *Dalton Trans.* **2008**, 2832.
(45) Chen, H.; Bartlett, R. A.; Olmstead, M. M.; Power, P. P.; Shoner, S. C. *J. Am. Chem. Soc.* **1990**, *112*, 1048.
(46) Bartlett, R. A.; Power, P. P. *J. Am. Chem. Soc.* **1987**, *109*, 7563.

Table 3. Magnetic Properties from Curie−Weiss Law Fits

cpd.	field T	temperature range, K	Nα	θ, K	C, Emu K/mol	μ_{eff}, μ_B	S
1	0.001	2−320	0	0.77(5)	4.17(10)	5.78(15)	5/2
2	0.001	2−320	0.000090	−2.20(6)	3.58(10)	5.36(15)	2
3	0.001	2−150		1.346	0.387	1.76	1/2
		250−320		−82	3.456	4.65[a]	3/2
	0.01	2−150		1.416	0.390	1.77	1/2
		250−320		−58	3.298	4.70[a]	3/2

[a] Calculated at 300 K from $\mu_{eff} = 2.828(x_M T)^{1/2}$.

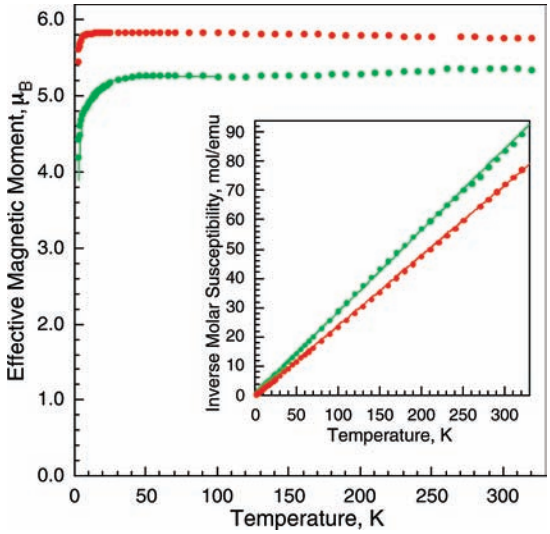

Figure 4. Temperature dependence of the effective magnetic moment of **1**, red, and **2**, green. The parameters for the fit of **2** shown between 2 and 100 K are $S = 2$, $g = 2.15$, and $D = 6$ cm^{-1}. Inset: the inverse molar magnetic susceptibility of **1** and **2** and their corresponding Curie−Weiss law fits.

The structure of **3** was determined by X-ray crystallography at both 90(2) K (**3a**) and 240(2) K (**3b**), and the structures are illustrated in panels a and b of Figure 3, respectively. The structural data for both forms are given in Table 2. It is noteworthy that the incipient structural change from the high spin, high temperature form (**3b**) to the low spin, low temperature form (**3a**) is discernible even at 240 K. At this temperature, the cobalt center is disordered over two positions. The main component is structure **3b**, which has 95% occupancy (the other 5% is structure **3a**), and is similar to those of **1** and **2** at 90 K. The cobalt center is coordinated to the aryl and arylamido ligands in a manner similar to that in **1** and **2**, and it interacts with the *ipso* carbon (C(37) of the flanking -C_6H_2-2,4,6-Me_3 ring at a distance of 2.393(2) Å which is considerably longer than the Co(1)−C(37) distance (2.077(3) Å) in the low spin form **3a** (see below). The Co(1)−C9(1) (1.992(2) Å) and Co(1)−N(1) (1.880(2) Å) distances are similar to those previously observed in the diaryl $CoAr_2^{\#}$ (2.001(3) Å)[37] and in the amides Co(N-(Mes)$BMes_2)_2$ (1.910(3) Å)[45] and Co(N($SiMe_3Ph_2)_2)_2$ (1.901(3) Å).[46] The C(1)−Co-N angle is 133.90(6)°, which lies between 127.1(2)° in Co(N(Ph)$B(Mes)_2)_2$[45] and 140.0(1)° in Co(N($SiMePh_2)_2)_2$.[45] The geometry of the minor 5% component has a structure that is the same as that observed for **3a** at 90(2) K. The major structural difference is that at the low temperature there is a strong cobalt-η^6 interaction with one of the flanking -C_6H_2-2,4,6-Me_3 rings instead of the weaker M---C interaction observed in (**3b**). The Co-centroid

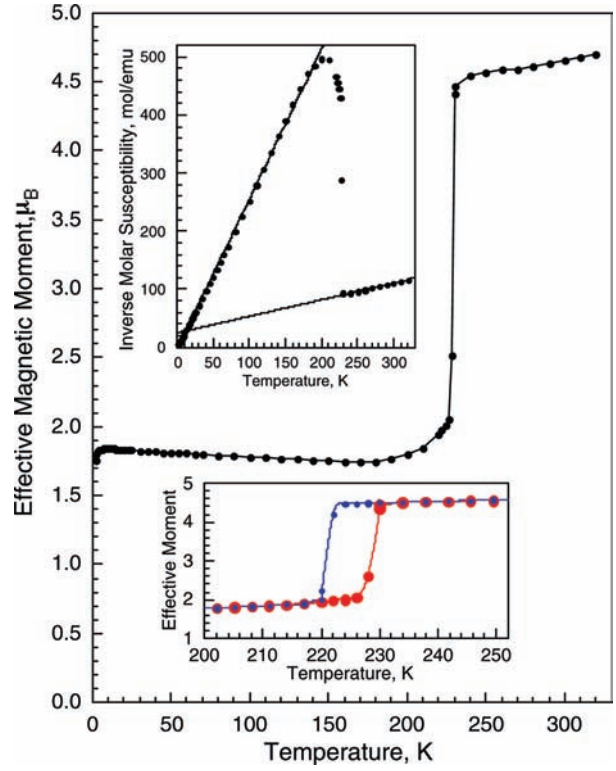

Figure 5. Temperature dependence of the effective magnetic moment of **3** obtained upon warming. Upper inset: the inverse molar magnetic susceptibility of **3** obtained upon warming and its corresponding Curie−Weiss law fit. Lower inset: The hysteresis in the effective magnetic moment of **3** observed upon warming, red, and cooling, blue.

distance is 1.636(3) Å, which is shorter than that in Ar′CoCoAr′ (1.7638(16) Å),[47] but is in the previously observed range of 1.561 to 1.766 Å.[48] The strong interaction causes the C(1)−Co-N(1) bending angle 101.75(11)° to be much narrower than the 133.90(6)° observed at 240(2) K. The strong Co-η^6-arene interaction is consistent with calculations for first row transition metal-arene interactions, which show that they are often stronger for cobalt.[49] The Co(1)−C(1) (1.977(1) Å) and Co(1)−N91) (1.875(3) Å) σ-bonded distances are marginally shorter than those in **3b** consistent with the low spin of the cobalt center. However, all the σ-bond lengths involving the transition metals (M−C(*ipso* carbon of the aryl) and the M−N distance) decrease in the sequence Mn > Fe > Co, and this is in agreement with the decrease in the size of these metals.[44,50] The C(32)−C(37) distances in **3a** and **3b**, as well as in **1** and **2**, are essentially the same and show no significant change from that of C(36)−C(46), which is the corresponding C−C distance of the non-interacting flanking -C_6H_2-2,4,6-Me_3 ring. Although the secondary M---C interactions in the four structures induce

(47) Nguyen, T.; Merrill, A.; Ni, C.; Lei, H.; Fettinger, J. C.; Ellis, B. D.; Long, G. J.; Brynda, M.; Power, P. P. *Angew. Chem., Int. Ed.* **2008**, *47*, 9115.
(48) Co-centroid distance of 31 Co-arene (benzene or toluene) complexes from Cambridge database (version 5.29, Feb, 2008).
(49) (a) Pandey, R.; Rao, B. K.; Jena, P.; Blanco, M. A. *J. Am. Chem. Soc.* **2001**, *123*, 3799. (b) Jaeger, T. D.; van Heijnsbergen, D.; Klippenstein, S. J.; von Helden, G.; Meijer, G.; Duncan, M. A. *J. Am. Chem. Soc.* **2004**, *126*, 10981. (c) La Macchia, G.; Gagliardi, L.; Power, P. P.; Brynda, M. *J. Am. Chem. Soc.* **2008**, *130*, 5105.
(50) Emsley, J. *The Elements*; Oxford University Press: Oxford, 1998.

considerable bending in their geometries, there are only relatively small effects on other structural parameters. Also, the M---C interaction with the flanking rings produce little structural change within the interacting rings. The N−C(31) distances in all four complexes remain essentially the same and marginally shorter than the C−N (1.396(3) Å) distance in the corresponding terphenyl aniline.[51]

Magnetism. Magnetic susceptibility studies were carried out on crystalline samples of **1**−**3** using a SQUID magnetometer. A diamagnetic correction[52] of −0.000571, −0.000533, and −0.000532, emu/mol, obtained from tables of Pascal's constants, have been applied to the measured susceptibility of **1**−**3**. As would be expected from the structures of **1**−**3**, these complexes are magnetically dilute and exhibit paramagnetic behavior, except perhaps rather low temperatures. The results[53] of a Curie−Weiss law fit of the inverse molar susceptibility of compounds **1**−**3** are given in Table 3.

The temperature dependence of the effective magnetic moments, μ_{eff}, and the inverse molar magnetic susceptibilities of **1** and **2** are shown in Figure 4; for each complex the magnetic properties are fully consistent with the presence of the expected high-spin manganese(II) and high-spin iron(II) ions. The effective magnetic moment of **1** is less than the expected 5.92 μ_B ($S = 5/2$) probably as a result of the presence of the diamagnetic impurities in the sample. The very small decrease in the μ_{eff} of **1** below about 5 K may be due to the onset of very weak long-range antiferromagnetic ordering; no attempt has been made to model this small decrease because of the presence of probably impurities. The μ_{eff} for **2** is 5.36 μ_B, which is significantly more than the spin only value 4.90 μ_B ($S = 2$), indicates a considerable orbital contribution to the effective magnetic moment and is consistent with incomplete quenching of the high orbital moment observed in a strictly linear, two coordinate Fe(II) species such as $Fe(C(SiMe_3)_3)_2$.[54] The decrease in μ_{eff} of **2** below about 50 K, see Figure 4, is predominantly due to zero-field splitting; a fit between 2 and 100 K with $S = 2$ yields $g = 2.1(52)$ and $D = 6(1)$ cm^{-1} values that are typical for high spin iron(II) in a distorted coordination environment.

The magnetic properties of **3** are especially interesting, see Figure 5, because they indicate that the cobalt(II) ion in this complex undergoes an electronic spin-state transition from the low-spin, $S = 1/2$, state below 229 K (**3a**) to the high-spin, $S = 3/2$ state (**3b**) above this temperature; as expected the results obtained at a 0.01 and 0.001 T applied field are virtually identical, which is in agreement with the structural change of **3** at 240 K. As is often the case for an electronic spin-state crossover, the transition exhibits an about 8 K hysteresis upon warming and cooling, which is shown in the lower inset to Figure 5. The presence of this hysteresis indicates that the transition is probably first-order. The magnitude and the small decrease in the observed μ_{eff} of **3** upon cooling from 320 to 230 K results, no doubt, from either the influence of spin−orbit coupling or the imminent onset of further cooling of the spin state crossover; because of this spin-state crossover it is not possible to evaluate the relative importance of these influences. Spin-state crossover in cobalt(II) systems has been well studied; however, the majority of those examined concern multidentate ligand complexes with six-coordination, or less commonly five-coordination, at cobalt.[55] In this case it is associated with a change in the effective coordination number from quasi three-coordinate in **3a** to quasi five-coordinate in **3b**.[55]

Conclusions

In summary, complexes **1**−**3** represent rare examples of monomeric, heteroleptic, open-shell Mn(II), Fe(II), and Co(II) amido complexes. Their synthesis is made possible by the availability of terphenyl stabilized aryl metal halide starting materials. The low spin configuration of **3** at low temperature (< ca. 229 K, i.e., **3a**) is consistent with the strong Co-η^6-arene interaction, and the high spin configuration of **(3b)** at high temperature is consistent with the lower effective coordination number of the metal as demonstrated by X-ray crystallography.

Acknowledgment. We thank the National Science Foundation (Grant CHE-0641020) and Peter Klavins for assistance in magnetization measurements.

Supporting Information Available: The crystallographic data for **1**−**3**. This material is available free of charge via the Internet at http://pubs.acs.org.

IC801660A

(51) Wright, R. J.; Steiner, J.; Beaini, S.; Power, P. P. *Inorg. Chim. Acta* **2006**, *359*, 1939.
(52) The diamagnetic corrections are believed to be accurate to at least ±10% of the value given and are probably more accurate. See Bain, G. A.; Berry, J. F. *J. Chem. Educ.* **2008**, *85*, 532.
(53) The rather higher than expected errors reported in Table 3 arise predominately from the difficulty in accurately determining the exact mass of the sample placed in a sealed quartz tube under dry nitrogen inside a Vacuum Atmospheres glove box. It is estimated that this error should be no more than 10% of the mass and is probably less.
(54) Reiff, W. M.; LaPointe, A. M.; Whitten, E. H. *J. Am. Chem. Soc.* **2004**, *126*, 10206.
(55) Goodwin, H. A. *Top. Curr. Chem.* **2004**, *234*, 23.
(56) Alvarez, S.; Cirena, J. *Angew. Chem., Int. Ed.* **2006**, *45*, 3012.